Global and Planetary Change 67 (2009) 117–128

Contents lists available at ScienceDirect

Global and Planetary Change

journal homepage: www.elsevier.com/locate/gloplacha

The impact of agricultural intensification and irrigation on land–atmosphere interactions and Indian monsoon precipitation — A mesoscale modeling perspective

E.M. Douglas [a,*], A. Beltrán-Przekurat [b], D. Niyogi [c], R.A. Pielke Sr. [b], C.J. Vörösmarty [d]

[a] University of Massachusetts, Boston, 100 Morrissey Blvd. Boston, MA 02125-3393, United States
[b] University of Colorado at Boulder, 1540 30th St, Boulder, CO 80309, United States
[c] Purdue University, 1088 Freehafer Hall, West Lafayette, IN 47907-108, United States
[d] University of New Hampshire, 39 College Rd. Durham, NH 03824, United States

ARTICLE INFO

Article history:
Accepted 8 February 2008
Available online 3 January 2009

Keywords:
irrigation
Indian monsoon
Regional Atmospheric Modeling System
agriculture
Land Use Land Cover Change

ABSTRACT

Using the Regional Atmospheric Modeling System (RAMS) we show that agricultural intensification and irrigation can modify the surface moisture and energy distribution, which alters the boundary layer and regional convergence, mesoscale convection, and precipitation patterns over the Indian monsoon region. Four experiments were conducted to simulate a rain event from 16 to 20 July 2002 over the Indian region: (i) a control with Global Land Cover land use and observed Normalized Difference Vegetation Index, (ii) an irrigated crop scenario, (iii) a non-irrigated crop scenario, and (iv) a scenario for potential (natural) vegetation. Results indicate that even under active monsoon conditions, the simulated surface energy and moisture flux over the Indian monsoon region are sensitive to the irrigation intensity and this effect is more pronounced than the impact of land use change from the potential vegetation to the agricultural landscape. When model outputs were averaged over the south Asia model domain, a statistically significant decrease in mean sensible heat flux between the potential vegetation and the irrigated agriculture scenarios of 11.7 Wm^{-2} was found. Changes in latent heat fluxes ranging from −20.6 to +37.2 Wm^{-2} (−26% to +24%) and sensible heat fluxes ranging −87.5 to +4.4 Wm^{-2} (−77% to +8%) fluxes were found when model outputs were averaged over Indian states. Decreases in sensible heat in the states of Punjab (87.5 Wm^{-2} or 77%) and Haryana (65.3 Wm^{-2} or 85%) were found to be statistically significant at the 95% confidence level. Irrigation increased the regional moisture flux which in turn modified the convective available potential energy. This caused a reduction in the surface temperature and led to a modified regional circulation pattern and changes in mesoscale precipitation. These agricultural changes, including irrigation modify the mesoscale convection and rain patterns in the Indian monsoon region. These regional changes in land use need to be considered in improved weather forecasting as well as multi-decadal climate variability and change assessments.

1. Introduction

Individuals and societies have always been vulnerable to weather extremes and rapid shifts in climate. But over the last few decades, evidence is growing that weather patterns and climate stability are vulnerable to humans as well. For instance, there is a growing consensus within the scientific community that human activities have played a key role in causing, or at least altering, the pace at which climate is changing. Although much of the current research focus has been on the direct effects of human activities on atmospheric composition, there is also mounting evidence that human-induced landscape changes can affect atmospheric processes from local to regional weather patterns (Cotton and Pielke, 2007; Pielke et al., 2002; Alpert et al., 2006) and climate variability (National Research Council, 2005; Kabat et al., 2004; Pielke et al., 2007a,b). Feddema et al. (2005) showed that the transient climate modeling based on the Intergovernmental Panel on Climate Change (IPCC) Special Report on Emissions Scenarios (SRES) lead to different regional climates when the impact of land cover changes are considered in addition to the SRES forcing alone. Gordon et al. (2005) evaluated the effects of land cover change on water vapor flows globally. They report that irrigated agriculture has increased global vapor flows by about 2600 $km^3\ yr^{-1}$, which is more than twice that of estimated global consumptive irrigation water losses (~1200 $km^3\ yr^{-1}$; Vörösmarty et al., 2005). Irrigation has been shown to significantly affect local and regional climate in the United States (e.g. Barnston and Schickedanz, 1984; Adegoke et al., 2003; Pielke, 2001). In the U.S., land cover change over the last 290 years has lead to a weak warming along the Atlantic coast and a strong cooling of more than 1 K over the Midwest and Great Plains region (Roy et al., 2003). Some reduction in precipitation due to changes in large-scale moisture advection has also occurred over the

* Corresponding author. Environmental, Earth and Ocean Sciences, 100 Morrissey Blvd, University of Massachusetts, Boston, Boston, MA 02125, United States. Tel.: +1 617 287 7437; fax: +1 617 287 7474.
E-mail address: ellen.douglas@umb.edu (E.M. Douglas).

0921-8181/$ – see front matter © 2008 Elsevier B.V. All rights reserved.
doi:10.1016/j.gloplacha.2008.12.007

Midwest. Extensive agricultural conversion in southern Florida has resulted in reduced precipitation and redistributed latent heat flux and atmospheric water vapor (Marshall et al., 2004a,b). Such changes can result in increased vulnerability to human populations.

The Indian subcontinent is a particularly interesting region for studying human–land–atmosphere interactions because it is home to one-sixth of the world's population, most of which rely very heavily on the summer monsoon rains for their survival. Gupta et al. (2006) document the rise and fall of agriculture and Indian societies in response to changes in the Indian monsoon. In general, humans prospered and agriculture flourished during wet phases of the summer monsoon while periods of weak summer monsoons led to famine and population migration (Davis, 2001). Irrigated agriculture in India has been a key component of economic development and poverty alleviation (Bansil, 2004). From 1951 to 1997, gross irrigated areas expanded four fold, from 23 million to 90 million hectares. While the benefits of this expansion in agricultural productivity have been immediate, the environmental and social costs over the long term are becoming increasingly apparent as well. For instance, most of the water used for irrigation in India is drawn from deep ground water bore wells. As a result, groundwater stores in India, estimated at 432 billion cubic meters (BCM; CWC, 1998) have been declining by 20 cm/yr^{-1} in as many as 15 Indian states (Bansil, 2004); groundwater stores in most of these states are predicted to dry up by 2025 or sooner (Jha, 2001). In addition to the impacts of intensive irrigation on local to regional hydrology, Gordon et al. (2005) suggest that expanding irrigation on the Indian subcontinent may increase the risk for changes in the Asian monsoon system and, thus, impact food production capacities in other regions (such as sub-Saharan Africa). Studies such as Boucher et al. (2004) concluded that the addition of water vapor in dry regions results in a nonlinear increase in precipitable water at the regional scale, which is compensated by a decrease in other regions through changes in convection.

Within India, there is also evidence that intensive irrigation has lead to changes in precipitation patterns. Lohar and Pal (1995) report that mean monthly rainfall from 1983–1992 in West Bengal, India, is less than half that observed from 1973–1982. The doubling of the area covered by summer paddy crops (mostly along the coast) over this time frame is a possible cause. Two-dimensional numerical simulations indicate that wetter soils along the coast reduce the temperature gradient between the land and the sea, hence weakening the sea-breeze circulation and reducing convective rainfall, which is a significant source of localized heavy precipitation rainfall in the coastal area.

Besides the obvious environmental and socioeconomic impacts that could result from changes in the Indian monsoon, Zickfeld et al. (2005) show that any perturbation in the radiative budget over the sub-continent can weaken the driving pressure gradient and

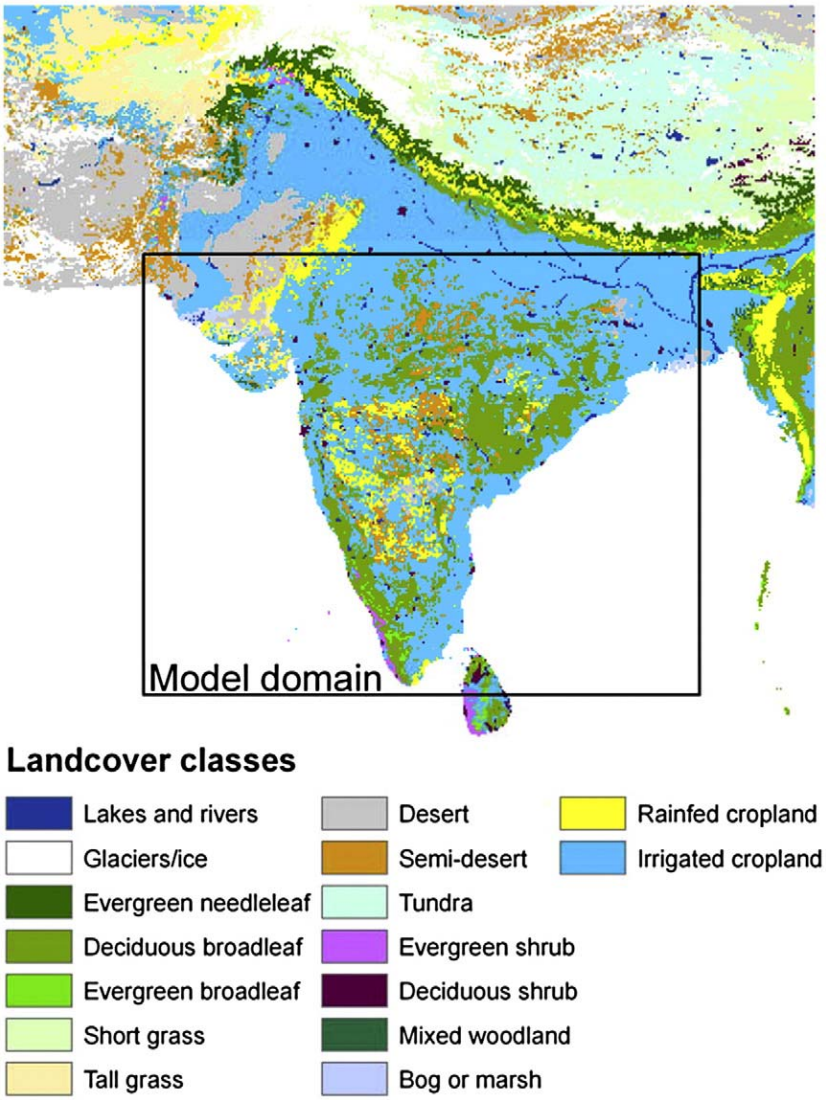

Fig. 1. Current state of land cover in India as represented by the GLC2000 land cover dataset. The model domain was constrained to peninsular India in order to reduce boundary effects due to the Himalayan Mountains.

potentially destabilize the summer monsoon circulation. They show that summer precipitation over India has two stable states: the current wet state (ranging from 4–10 mm d^{-1}) and a dry state (<1 mm d^{-1}). An increase in the present-day planetary albedo from 0.47 to 0.50 would decrease precipitation from around 8 mm d^{-1} to 4 mm d^{-1}. Any further increase would result in the destabilization of the summer monsoon regime and a settling to the second, dry state. Once this dry state is achieved, hysteresis in the system would require that the planetary albedo be reduced to 0.48 (not 0.50) before the potential for returning to the wet state can be reached. Thus, land surface changes could have a profound impact on the monsoon system.

Douglas et al. (2006) explored changes in evapotranspiration and latent heat fluxes due to agricultural conversion in India. They compared vapor fluxes (estimated evaporation and transpiration) from pre-agricultural and contemporary land covers and found that mean annual vapor fluxes have increased by 17% (340 km^3) with a 7% increase (117 km^3) in the wet season and a 55% increase (223 km^3) in the dry season. Two-thirds of this increase was attributed to irrigation, with groundwater-based irrigation contributing 14% and 35% of the vapor fluxes in the wet and dry seasons, respectively.

The objectives of this paper are to study the effect of changes in agricultural land-use change and irrigation using a three-dimensional numerical model, the Regional Atmospheric Modeling System (RAMS), in order to extend the findings of Douglas et al. (2006) and to further investigate changes in the energy budget and in land–atmosphere interactions attributable to irrigated agriculture.

2. Methodology

2.1. Landcover

Fig. 1 shows the contemporary state of land cover in India as represented by the South Asia region GLC2000 dataset (Agrawal et al., 2003) aggregated to a 5-minute (~9 km) spatial grid mapping. Each 5-minute grid cell represents the majority land cover as quantified from the original 1-km grid increment dataset. Fig. 1 also shows that the contemporary Indian landscape is made up of a rich mosaic of natural vegetation and human land uses. In order to separate out the influence of agricultural conversion and particularly the effects of irrigated agriculture on land–atmosphere interactions, we devised the three land cover datasets shown in Fig. 2: (a) pre-agricultural (POT),

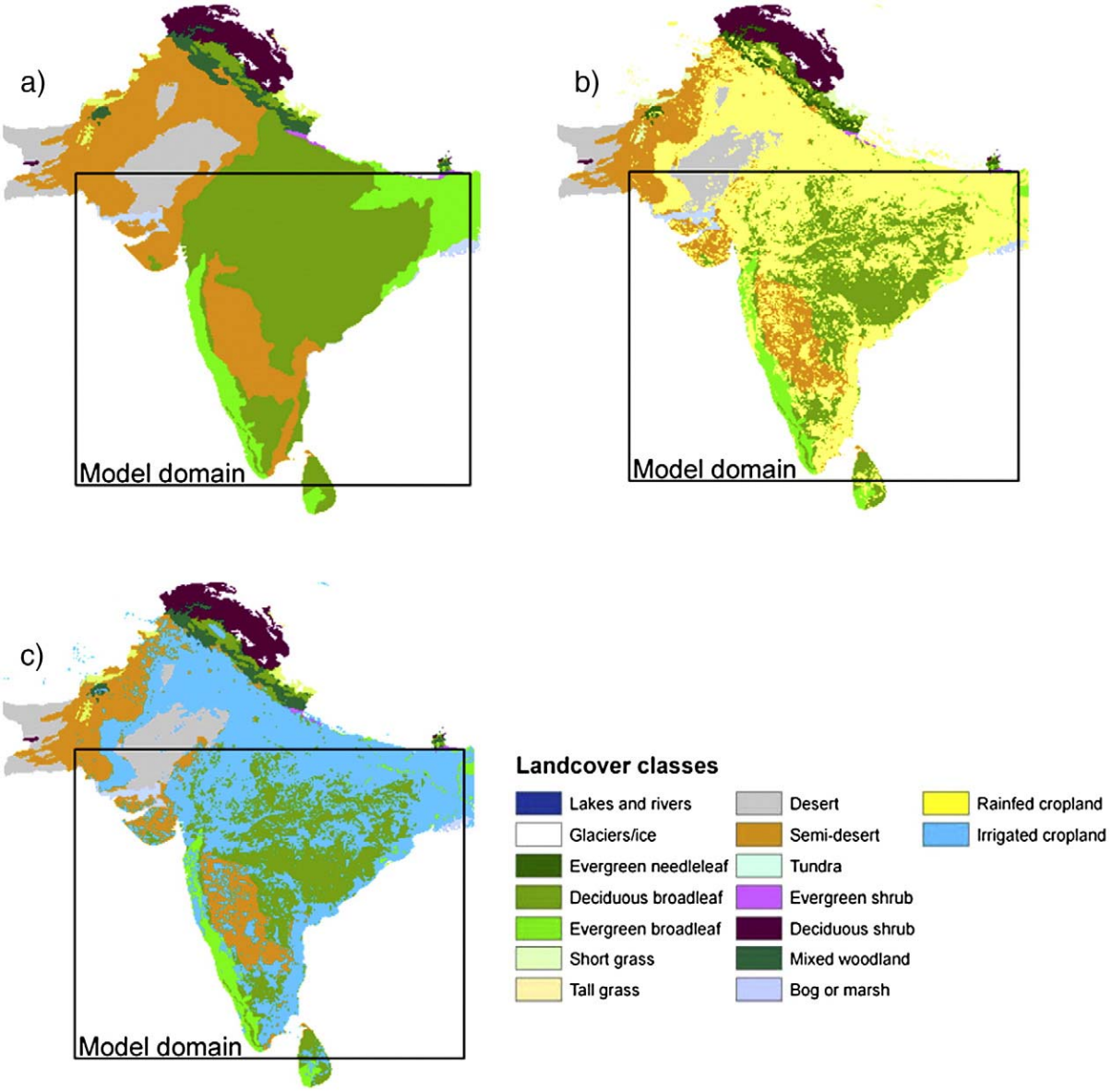

Fig. 2. Land cover scenarios used in this study: a) potential (pre-agricultural or POT) land cover, b) rainfed cropland (CRP) and c) irrigated cropland (IRR).

(b) rainfed agriculture (CRP), and (c) irrigated agriculture (IRR). The pre-agricultural landcover was derived from the World Wildlife Fund (WWF) Terrestrial Ecoregions of the World map (Olson et al., 2001). This is a global map of ecoregions containing more that 800 ecosystems which are classified into biogeographical realms and biomes. WWF defines ecoregions as 'relatively large units of land containing a distinct assemblage of natural communities and species, with boundaries that approximate the original extent of natural communities prior to major land-use change'. Hence ecoregions reflect 'potential' land-cover and do not take into account human land uses or conversions. The ecoregion classifications were converted to RAMS land-cover classes using the ecoregion descriptions (http://www.worldwildlife.org/science/ecoregions/biomes.cfm).

As can be seen in Fig. 1, almost all cropland in the Indian domain shown in the GLC2000 database is irrigated. For the rainfed cropland scenario (CRP), we selected any grid cell in which the majority land cover was cropland (rainfed or irrigated) and overlaid it onto the potential land cover map. For a 5-minute grid cell to be specified as irrigated cropland, we selected a threshold of >60% irrigated cropland. In this way, we retained the spatial distribution of irrigated cropland in the original high resolution dataset while minimizing the over-estimation of irrigation extent. For the irrigated cropland scenario (IRR), we selected grid cells specified as irrigated cropland (from Fig. 1) and overlaid them onto the potential land cover. The GLC2000 landcover dataset provides information on the land surface percentage that is irrigated and does not provide information on the source of irrigation water (i.e. groundwater, canal, or surface water), hence we evaluated the impacts of irrigation in general and not by source.

2.2. Atmospheric model

For this analysis we used the Regional Atmospheric Modeling System version 4.3 (RAMS). RAMS is a general-purpose, atmospheric-simulation model that includes the equations of motion, heat, moisture and continuity in a terrain-following coordinate system. It is a three dimensional, non-hydrostatic atmospheric modeling system. RAMS is most often used as a limited area model, and many of its parameterizations have been designed for mesoscale or high resolution cloud scale grids. RAMS has also been utilized extensively for studying land use change effects on regional climate (e.g. see Pielke et al., 1992; Cotton et al., 2003 for overviews). RAMS also includes a soil–vegetation–atmosphere transfer scheme, the Land Ecosystem-Atmosphere Feedback model version 2, (LEAF-2) (Walko et al., 2000) that represents the storage and exchange of heat and moisture associated with the vegetation and canopy air and soil. The implementation of LEAF-2 within RAMS allows multiple surface types to coexist beneath a single grid-resolved column of air.

The model domain (box in Figs. 1 and 2), centered at (15.5°N, 78.0°E), was discretized horizontally into 25 km grid cells (24×103 grid cells). There were 34 vertical levels with an average thickness of 140 m at the lower levels, stretching to 1 km from approximately 8.5 km to the domain top at 20 km. The soil model had 8 soil layers, with the bottom layer at 3.0 m. The Chen and Cotton (1983) radiation scheme were used for short- and long-wave radiation fluxes. Convective precipitation was parameterized using the Kain–Fritsch convective parameterization (Castro et al., 2002; Kain, 2004) which replaced the standard Kuo scheme in this RAMS version. The surface layer was parameterized following similarity theory. The Mellor and Yamada (1982) parameterization was used for vertical diffusion and the modified Smagorinsky (1963) scheme for horizontal diffusion. The lateral boundary conditions were those of Klemp and Wilhelmson (1978).

To study the impacts of land surface changes related to agriculture intensification and irrigation, a five-day period (16 to 20 July, 2002) during the summer monsoon was simulated. This period corresponds to a typical heavy rain episode over the Indian region and coincided with an intensive observational phase of a field experiment (Arabian Sea Monsoon Experiment, ARMEX, Rao and Sikka, 2005). Atmospheric lateral boundary forcing and initial atmospheric fields were provided by the European Centre for Medium-Range Weather Forecasts (ECMWF) 40-yr reanalysis (ERA-40) dataset (Uppala et al., 2005). The reanalysis data were assimilated every 6 hr, and ten grid points were used for the lateral boundary nudging. For internal nudging a 24-hr timescale was applied. Initial soil moisture conditions were taken from ERA40. Leaf area index (LAI) data were derived from the NASA Global Inventory Modeling and Mapping Studies (GIMMS) Normalized Difference Vegetation Index (NDVI) at 8 km resolution, for the 1–15 July 2002 period (Pinzón, 2002; Pinzón et al., 2004; Tucker et al., 2005). NDVI data were converted to LAI using the algorithm by Sellers et al. (1996) and held constant during the 5-day simulation. Table 1 lists the vegetation parameters used in RAMS to simulate the different land cover types.

Table 1
Vegetation parameter values used in RAMS to simulate the different land cover types.

Land cover type	Albedo	Emiss	z_0 (m)	z_{disp} (m)
Evergreen needleleaf forest	0.10	0.97	1.00	15
Deciduous needleleaf forest	0.10	0.95	1.00	20
Deciduous broadleaf forest	0.20	0.95	0.80	15
Evergreen broadleaf forest	0.15	0.95	2.00	20
Short grass	0.26	0.96	0.02	0.2
Tall grass	0.16	0.96	0.10	1
Desert	0.30	0.86	0.05	0.1
Semi-desert	0.25	0.96	0.10	0.5
Tundra	0.20	0.95	0.04	0.1
Evergreen shrub	0.10	0.97	0.10	1
Deciduous shrub	0.20	0.97	0.10	1
Mixed woodland	0.15	0.96	0.80	20
Crop/mixed farming	0.20	0.95	0.06	0.7
Irrigated crop	0.18	0.95	0.06	0.7

An initial experiment with the GLC2000 dataset was carried out, and used to validate RAMS simulated precipitation with a combination of station and satellite data. A gridded daily precipitation dataset, the GPCP 1°×1° (Huffman et al., 2001) was used. These data combine several satellite estimates plus rain gauge observations over land and oceans. The Tropical Rainfall Measuring Mission TRMM 3B24 V6 three hourly rainfall data with a footprint of 0.25°×0.25° were also used. Observed daily rain gauge precipitation from a total of 71 stations, 29 from the ARMEX field program and 42 from the Global Surface Summary of the Day Data Version 6, were also compared with simulated precipitation.

Domain-averaged bias, spatial correlation, and root-mean-squared-error (RMSE) were computed using the accumulated precipitation, with the GLC2000 dataset as land-cover, during the simulation period. The simulated precipitation, remapped to a 0.25°×0.25° grid, was compared to the TRMM dataset. The domain-averaged bias was 14.5 mm, calculated as mean GLC precipitation minus mean TRMM precipitation (41.8 mm–27.3 mm, respectively).

The spatial correlation (between the simulated and observed precipitation fields) was 0.59 (the model explained 34% of the variance). RMSE was quite high, at 41.6 mm, most likely due to differences in the spatial patterns of modeled versus observed precipitation. These values indicate that modeled precipitation tended to be overestimated and did not coincide spatially with observed precipitation in some areas. In the experiments, simulated precipitation was the result mainly of convective processes. Two convective schemes are currently available in the RAMS version: Kuo (Kuo, 1974; Molinari, 1985) and Kain–Fritsch (Kain, 2004; Castro et al., 2002). In general, simulated RAMS precipitation tends to be overestimated throughout the entire domain (Saleeby and Cotton, 2004; Beltrán 2005; Castro et al., 2005, 2007). Simulated precipitation using the Kuo scheme had a lower bias (spatial average precipitation was 26.3 mm, therefore the bias compared to TRMM was −1.0 mm) but

the spatial distribution was not as well represented as with the Kain–Fritch scheme. Simulated precipitation is also controlled by the model set-up, such as nudging timescale and the number of nudging points at the boundaries (Castro et al., 2007) and lateral boundary conditions (i.e. global reanalysis used, like NCEP or ERA-40 dataset, Beltrán 2005).

To analyze the effects of land-use/land-cover changes including irrigation on the near-surface atmosphere, three additional simulations were performed. RAMS was used with the same configuration and initial conditions in all cases, except for the land cover dataset were the irrigated crop scenario (IRR), the non-irrigated crop scenario (CRP) and the potential vegetation (POT) scenario. To counteract the

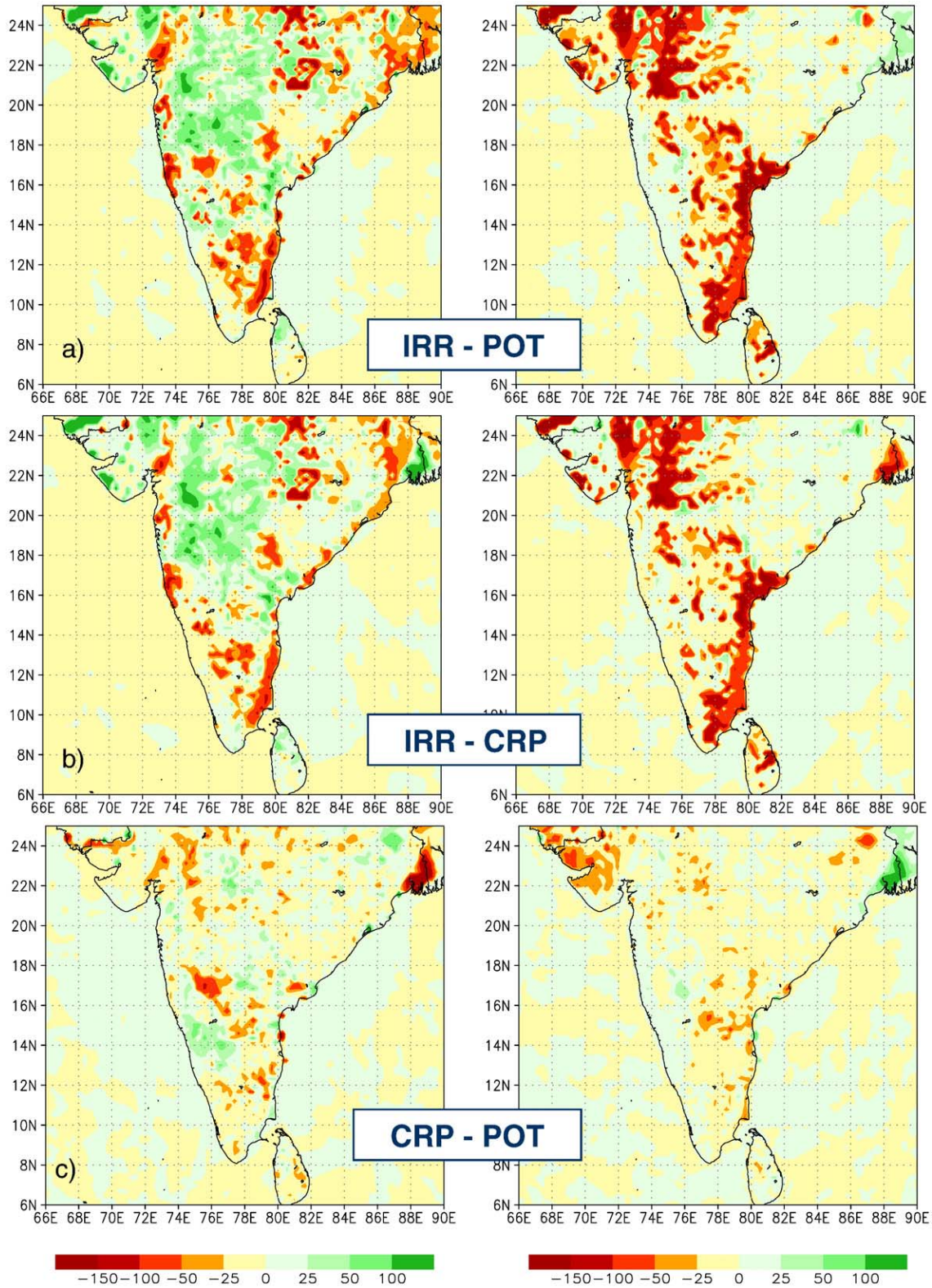

Fig. 3. Difference in latent heat (left column) and sensible heat (right column) (Wm^{-2}) between three land-cover change scenarios: a) potential landcover to irrigated cropland (IRR-POT), b) rainfed cropland to irrigated cropland (IRR-CRP) and c) potential landcover to rainfed cropland (CRP-POT).

fact that the model did not reproduce precipitation very well, we used the pre-agricultural land cover scenario (POT) as the baseline and compared differences between model outputs from the POT scenario and the other scenarios.

3. Results and discussion

3.1. Effects of landcover change on energy fluxes

The summer monsoon rainfall changes the moisture conditions over India. The influx of moisture from the summer monsoon transforms central and northern India from semi-arid conditions to humid conditions in less than a month's time, on average, as indicated by an analysis of the monthly Climate Moisture Index (CMI; Willmott and Feddema, 1992; not shown). Changes in the land surface in this region of India are abrupt and the atmosphere can reach a new equilibrium for surface energy within matter of weeks (Krishnamurti and Biswas, 2006).

Fig. 3 compares the differences in simulated surface energy budgets for the three land-cover scenarios and illustrates the impact of land-cover change on the partitioning of this energy between latent heat and sensible heat. The conversion of natural land cover (POT) to rainfed cropland (CRP) (CRP-POT, Fig. 3c) appears to have little effect on the surface energy budget for this monsoon rainfall case, except near the mouth of the Ganges River, where latent heat decreased 100–150 Wm^{-2} and sensible heat increased on the order of 100 Wm^{-2}. In this area, moist tropical forests were almost completely converted to agricultural land use. This decrease is likely due to the two orders of magnitude reduction in roughness height (z_0 in Table 1) between forest and agricultural land cover. The higher z_0 permits a greater exchange of latent heat flux for a given set of meteorological conditions. If the nature of the surface changes, the change in surface roughness will directly affect the exchange of latent and sensible heat fluxes (Pitman, 2003). For most of the rest of India, changes in latent and sensible heat fluxes were between ± 25 Wm^{-2}. However, major differences can be seen when irrigation is added to the landscape.

The conversion from CRP-IRR (Fig. 3b) and POT-IRR (Fig. 3a) both show decreases in sensible heat flux of 100 Wm^{-2} or more in the northwestern section of the model domain and along the southeastern coast. In these areas, changes from moist deciduous forest to cropland or irrigated land did not result in dramatic changes in albedo or roughness height (see Table 1). Instead, the changes in energy partitioning are likely due to the cooling effect of increased soil moisture, which in the model was set at saturation in irrigated cells.

Interestingly, while a broad region of the northwest shows increased latent heat fluxes due to irrigation, as would be expected, the southeastern coast shows a decrease in latent heat as well. Along the southeastern coast, the semi-desert was converted to agriculture, resulting in a 20% reduction in albedo and an order of magnitude reduction in roughness height. Although the reduction in albedo would result in an increase in net radiation (available energy) and the reduction in roughness height should yield an increase in partitioning to sensible heat, the dominant process appears to be the increased available soil moisture which resulted in an overall decrease in sensible heat. Douglas et al. (2006) found a similar pattern of increased and decreased latent heat fluxes when using a terrestrial water balance model (WBM; Vörösmarty et al., 1998) to evaluate changes in vapor and energy fluxes to the atmosphere using a similar land cover conversion scenario.

In response to changes in the partitioning of energy fluxes, the Bowen ratio progressively decreases from POT to CRP to IRR (Fig. 4), indicating that more of the available energy is going towards latent heating. In general, the most dramatic changes in energy fluxes and partitioning occur in the regions that were classified as arid landscapes according to the CMI (Willmott and Feddema, 1992). The Bowen ratio in north central India can vary with monsoon (Krishnamurti and Biswas, 2006), and the reduction in the Bowen ratio due to irrigation represents a significant alteration of the energy regime across much of India. The impacts of regional Bowen ratio change are

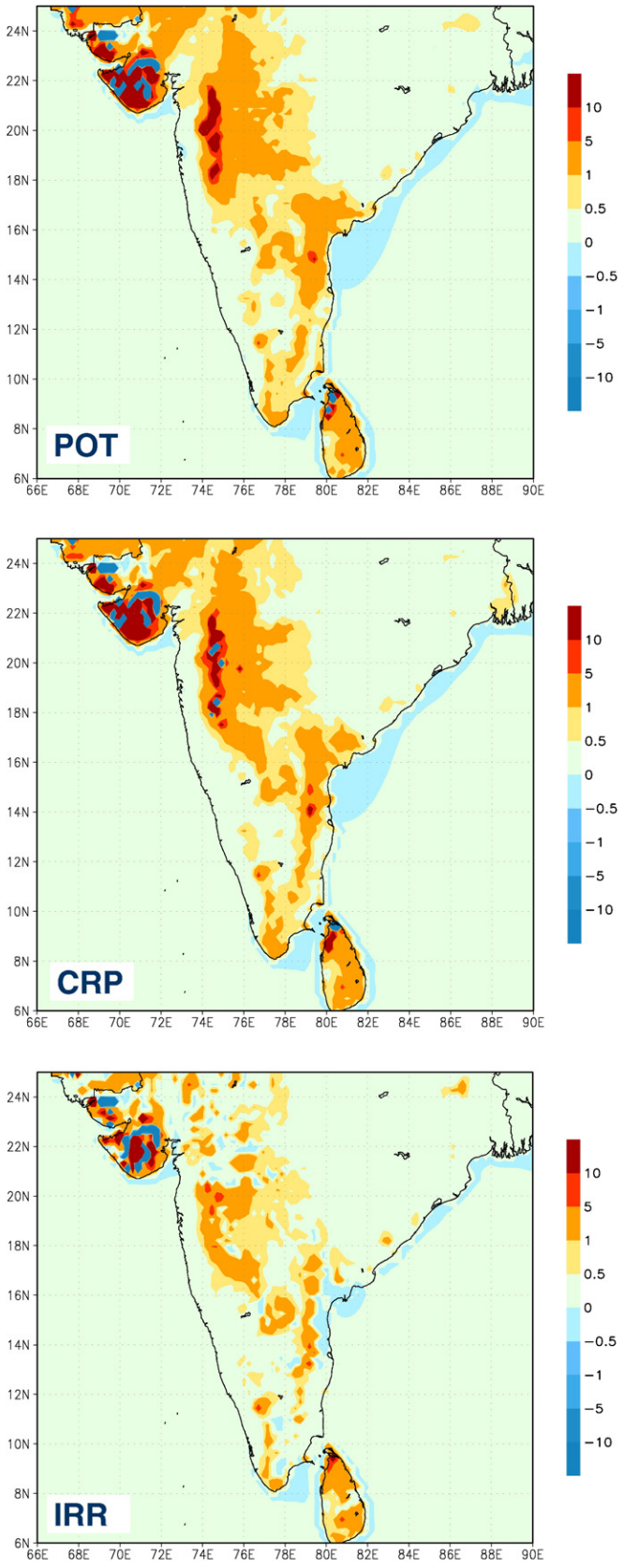

Fig. 4. Spatial distribution of the daytime Bowen ratio (sensible heat/latent heat) for the three land cover scenarios.

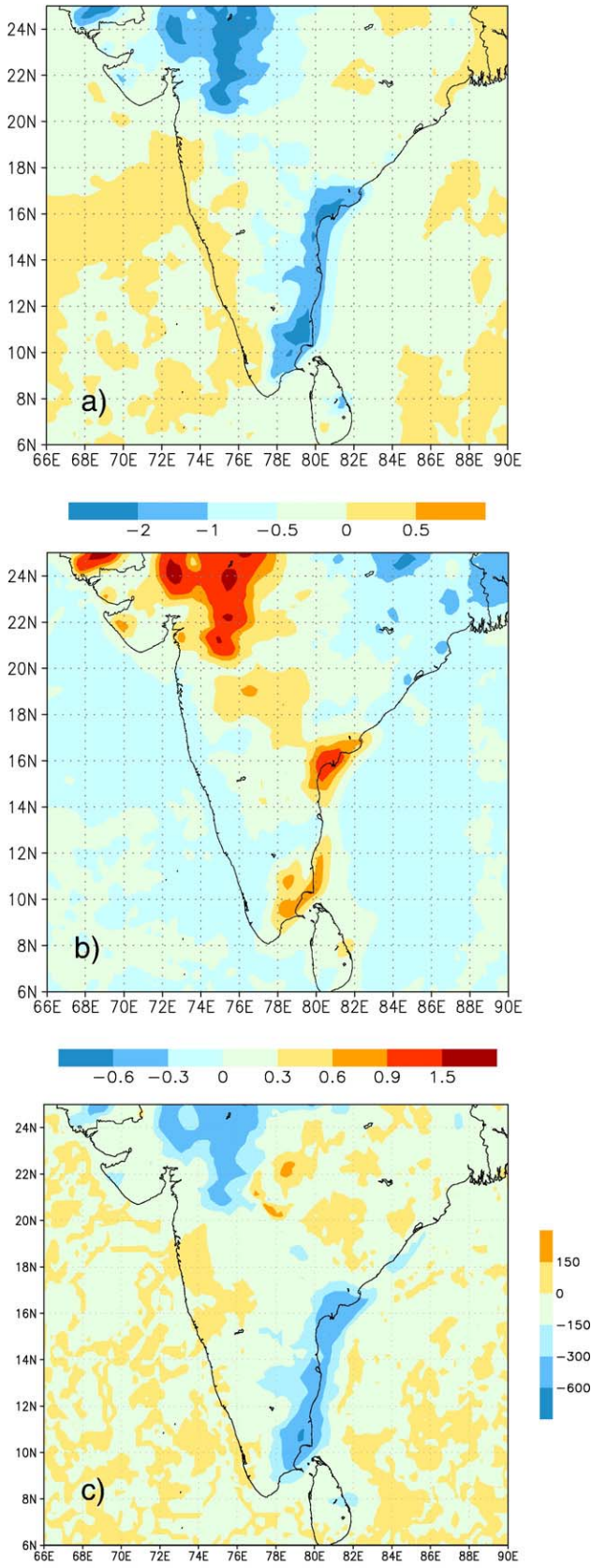

Fig. 5. Changes in a) temperature (°C), b) water vapor (g kg^{-1}) and c) planetary boundary layer height (m) due to conversion of potential landcover to irrigated cropland.

expected to effect regional circulation, boundary layer evolution, and mesoscale convection (Holt et al., 2006), and is discussed in the following sections.

3.2. Effects of landcover change on atmospheric conditions

A larger fraction of energy partitioned to latent heat fluxes can result in greater convective available potential energy (CAPE), as well as added water vapor to fuel deep convection, if suitable conditions exist (Pielke, 2001). A smaller fraction of sensible heat flux, however, will result in sufficiently weaker boundary layer convection such that the CAPE may not be realized as showers and thunderstorms. Physical evaporation is generally small in the non-irrigated areas such that deep convection that develops in these regions has transpiration as its primary land source of atmospheric moisture to add to the CAPE. In non-irrigated regions, net radiation will primarily be partitioned into sensible heat fluxes, as vapor fluxes into the atmosphere from water stressed vegetation will be negligible. However, irrigation will introduce significant latent heat fluxes resulting from the transpiration (and associated physical evaporation from the adjacent bare soils) of water vapor. If the irrigated areas are large enough (10 s of km on a side or larger), mesoscale circulations can develop associated

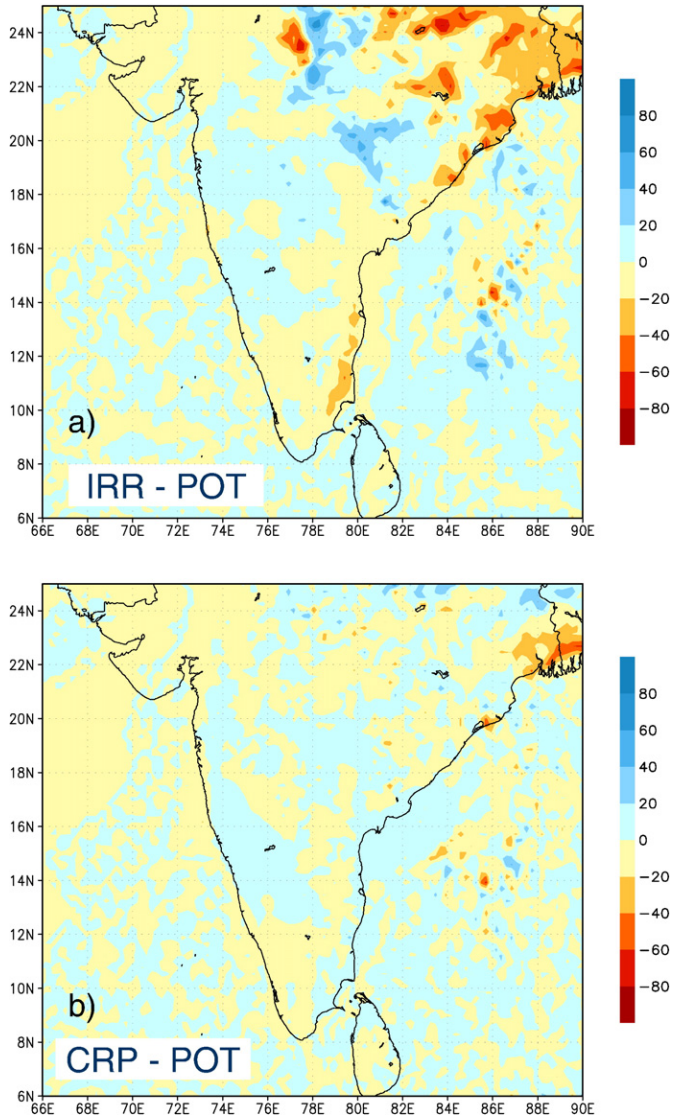

Fig. 6. Effect of land cover conversion from potential land cover to a) irrigated cropland and b) rainfed cropland on precipitation patterns (mm).

with boundary layer wind convergence between the dry and wet areas, similar to what occurs with sea breeze convergence zones (Pielke, 1974) and deforested areas (Avissar and Liu, 1996).

As shown in Fig. 5, the intensive irrigation in the northwest section of the model domain and along the southeast coast has suppressed the air temperature by 1 to 2 K (Fig. 5a) and has increased the water vapor content by about 1 g kg^{-1} (Fig. 5b) in the lower atmospheric model layers. It has also resulted in a suppression of the average daytime planetary boundary layer (PBL) from 2800 to 2100 m between the POT and IRR cases (Fig. 5c). Note that the PBL suppression in this 3D case is consistent to the 1-D atmospheric modeling experiment performed by Douglas et al. (2006), who reported that the depth of the summertime PBL was proportional to the sensible heat flux, and irrigation will lead to lowered boundary layer heights. While the change from potential vegetation to a rainfed agricultural landscape did affect the surface energy fluxes, the impact on the precipitation was not substantial, indicating that the more organized nature of irrigation and the enhanced source of surface moisture through irrigation appear to have more dramatic impact on the regional precipitation.

For most of India, the change from potential to rainfed cropland has resulted in a change in simulated precipitation of only ±20 mm (Fig. 6a). An exception is near the mouth of the Ganges, where conversion of moist tropical forest has resulted in a reduction in precipitation of 20–60 mm. This supports the findings of Lohar and Pal (1995), who suggested that irrigation in the South West Bengal region reduces the intensity of sea breeze activity, resulting in decreased thunderstorm activity and rainfall. The conversion to irrigated cropland has resulted in increased precipitation in some areas over the north central section of the model domain and decreased precipitation over northeastern section of the model domain. As previously noted, this appears to be somewhat of a terrain effect with lower precipitation occurring in low-lying the Ganges–Bramaputra basins and higher precipitation due to a ridge of higher terrain.

Fig. 7 shows the expected increase in CAPE resulting from the increased latent heat fluxes from irrigated cropland in the northwest. It also shows that CAPE is decreased in the extreme northwest corner of the domain, the northeast (near the mouth of the Ganges) and along the southeast coast, coincident with areas of dramatically reduced sensible heat fluxes shown in Fig. 3. These results indicate that the impact of irrigation on CAPE depends on how surface energy partitioning is affected. In arid regions (such as parts of northwestern and southeastern India), the predominant effect of irrigation appears to reduce CAPE due to the suppression of sensible heat fluxes.

3.3. Sensitivity analysis

In order to ascertain the effect of vertical and horizontal discretization and the timing of our analyses, we performed four ensemble sensitivity simulations: “dz” representing a decrease in the lowest average vertical thickness from 140 m to 70 m; “earlier” representing an earlier start of the simulations from July 16 to July 10, “dx” representing a decrease of grid cell spacing from 25 to 12 km and “larger”, in which the model domain was expanded to include the entire south Asian GLC2000 land cover domain. For each of these sensitivity experiments, we used the same three land cover scenarios (POT, CRP and IRR) as in the original simulations except for the “larger” experiment, which we only ran for the POT and IRR scenarios. Fig. 8 compares the mean values for latent and sensible heat (Wm^{-2}), precipitation (mm) and water vapor (g kg^{-1}) from each of the sensitivity run with the mean values from the original simulation results already discussed. Mean values represent averages over the entire domain. Error bars represent the 95% confidence intervals for

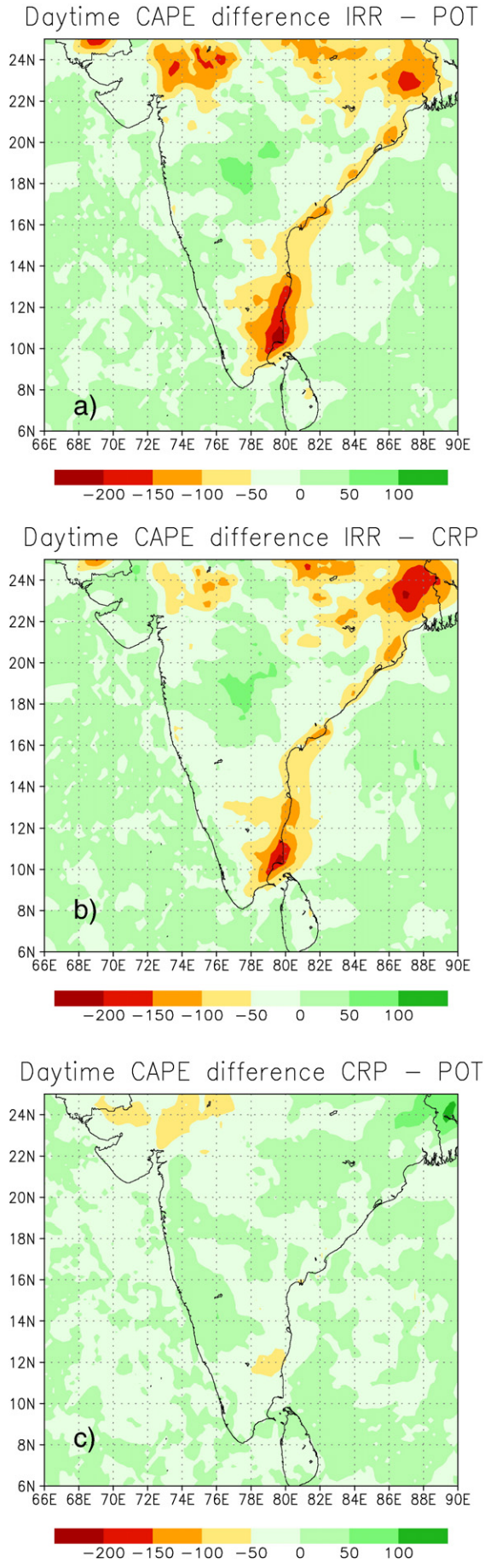

Fig. 7. Differences in convective available potential energy (CAPE) (J kg^{-1}) for the three landcover scenarios: a) potential to irrigated cropland, b) rainfed to irrigated cropland and c) potential to rainfed cropland.

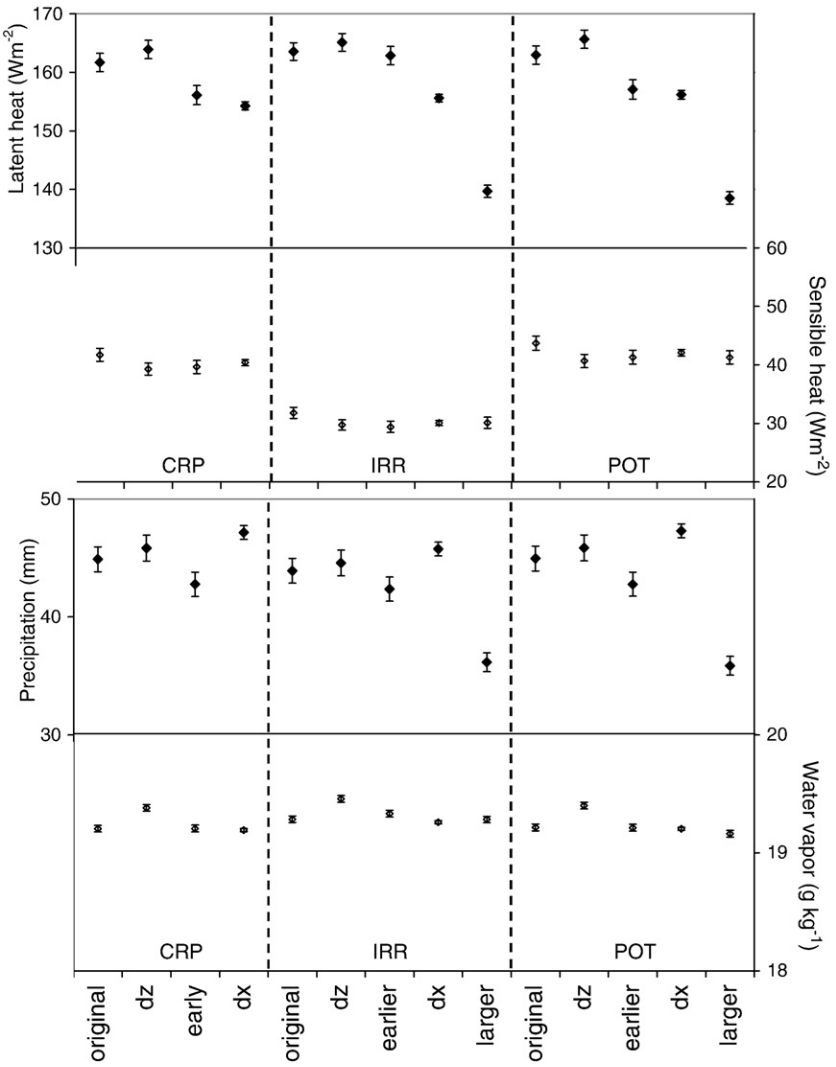

Fig. 8. Results of sensitivity analysis on domain-averaged latent heat, sensible heat, accumulated precipitation and water vapor. "dz" represents a change in vertical discretization (from 140 m to 70 m), "early" represents a shift in the start time of the simulations (from July 16 to July 10), and "dx" represents a reductions in grid cell size (from 25 to 12 km).

the mean. All statistics were computed over the original domain (represented by the box in Fig. 2).

Sensible heat (SH) and water vapor (VP) were the least sensitive model outputs. SH mean values from the sensitivity runs were lower and significantly different (at 95%) than the original run for all three scenarios. VP mean values were significantly higher for the "dz" run in each scenario; VP mean values were statistically similar for the other runs. Latent heat (LH) and precipitation (PR) were the most sensitive outputs in our analysis. Statistically significant differences were not observed between the original and "dz" runs for either LH or PR, but significant differences were observed between the "earlier" and "dx" runs for the CRP and POT scenarios. Interestingly, mean LH was not significantly different between the original, "dz", "earlier" and "dx" runs under the IRR scenario nor was mean PR significantly different between the original, "dx" and "earlier" runs. Spatial discretization had the most dramatic affect on LH and PR but not on SH and VP. Because of the observed sensitivity of some of the model outputs, we present the averages of LH, SH, PR and VP computed over the original, "dz", "earlier" and "dx" experiments in Table 2. We also computed 95% confidence intervals for these mean values (not shown). We did not include the "larger" results in the averages because of differences in terrain and boundary conditions.

Overall, SH was most dramatically influenced by a change in land cover, with a decrease of 11.7 Wm^{-2} (28%) between the POT and IRR scenarios. This decrease in SH for the IRR scenario was outside the 95% confidence interval for the mean SH flux for the POT scenario, indicating that this changes was statistically significant. A domain-averaged decrease in LH of 1.5 Wm^{-2} was observed between the POT and CRP scenarios; a domain-averaged increase in LH of 1.3 Wm^{-2} was observed between the POT and IRR scenarios. Both of these changes were less than 1% over the entire domain, however, Fig. 3 shows that these changes are much larger in the northwest and along the southeastern coast. Domain-averaged PR decreased by 1.1 mm

Table 2
Domain-average and scenario differences for latent heat, sensible heat, accumulated precipitation and water vapor for the POT, CRP and IRR land cover scenarios. Reported values represent averages of the original simulations and the sensitivity runs "dz", "earlier", "dx". We did not include the results of the "larger" runs because of differences in boundary conditions and terrain. Differences in sensible heat (bold and italicized) were greater than the 95% confidence intervals for the scenario averages, indicating that these differences are statistically significant.

	Land cover scenario			Differences between scenarios		
	POT	CRP	IRR	CRP-POT	IRR-POT	IRR-CRP
LH (Wm^{-2})	160.5	159.0	161.8	−1.5	1.3	2.8
SH (Wm^{-2})	41.9	40.3	30.3	***−1.7***	***−11.7***	***−10.0***
Precipitation (mm)	45.2	45.2	44.1	−0.1	−1.1	−1.0
Vapor (g/kg)	19.3	19.2	19.3	−0.01	0.08	0.09

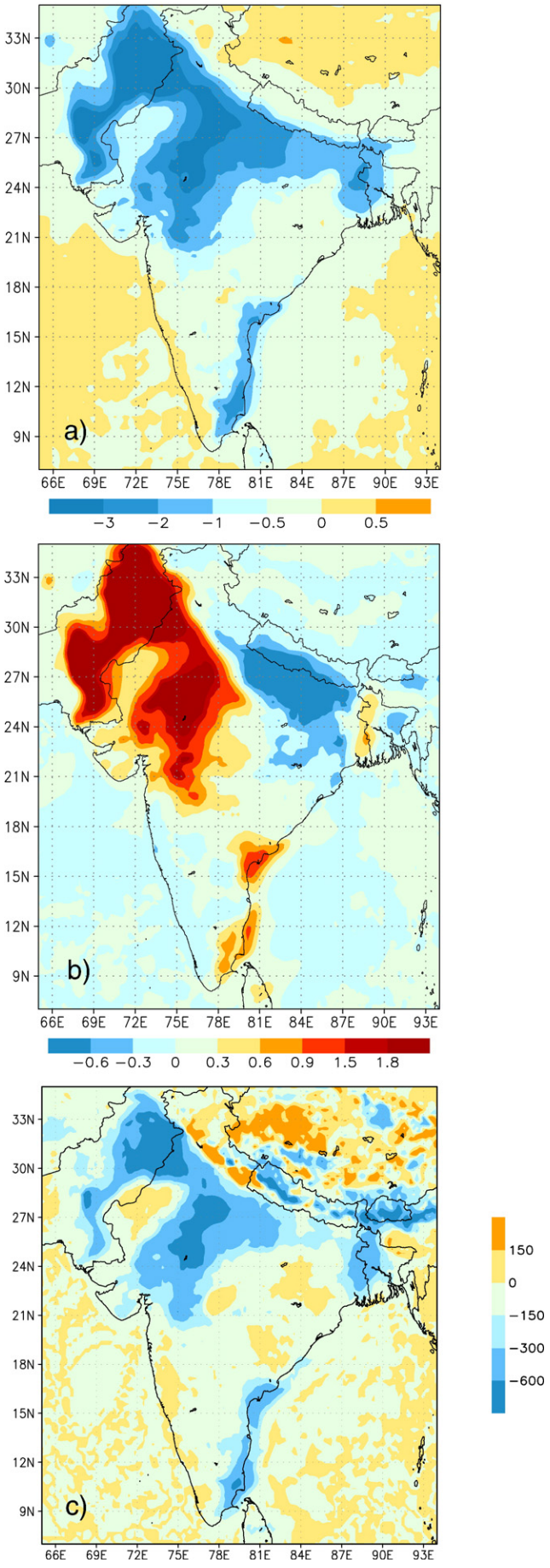

Table 3a
Summary of latent heat fluxes by Indian state estimated by RAMS over the larger domain. POT denotes the potential vegetation scenario, IRR denotes the irrigated agriculture scenario. Also included are seasonal and annual differences in latent heat fluxes between the potential and irrigated agriculture scenarios estimated by the water balance model (Douglas et al., 2006).

State[a]	RAMS latent heat (Wm^{-2})				WBM latent heat differences (Wm^{-2})		
	POT[b]	IRR[b]	Difference[c]	% Change[d]	Kharif	Rabi	Annual
Andhra Pradesh	176.8	182.2	5.4	3.1	11.0	4.8	8.2
Arunachal Pradesh	122.8	119.0	−3.8	−3.1	0.2	−1.3	−0.5
Assam	106.4	90.8	−15.5	−14.6	2.3	−11.1	−3.8
Bihar	198.7	198.5	−0.2	−0.1	0.0	11.0	5.0
Gujarat	123.9	136.0	12.1	9.8	13.1	6.7	10.3
Haryana	135.3	142.6	7.4	5.4	54.7	95.7	73.2
Himachal Pradesh	85.8	89.0	3.2	3.7	0.3	−0.8	−0.2
Jammu and Kashmir	178.9	169.4	−9.4	−5.3	1.4	−1.7	0.0
Karnataka	217.1	200.4	−16.7	−7.7	7.0	−4.6	1.8
Kerala	204.3	199.9	−4.4	−2.2	2.9	−10.6	−3.2
Madhya Pradesh	152.9	158.2	5.3	3.4	−2.0	25.5	10.4
Maharashtra	127.4	141.8	14.4	11.3	−0.6	11.6	4.9
Manipur	234.4	232.4	−2.1	−0.9	1.1	−3.5	−1.0
Meghalaya	107.0	125.6	18.6	17.3	2.6	−22.9	−8.9
Mizoram	281.0	268.7	−12.3	−4.4	0.2	−2.7	−1.1
Nagaland	225.9	224.0	−1.9	−0.8	0.9	−7.7	−3.0
Orissa	241.2	231.0	−10.2	−4.2	2.0	−7.7	−2.4
Punjab	157.3	194.5	37.2	23.7	36.7	92.1	61.7
Rajasthan	113.2	137.2	24.0	21.2	10.8	12.5	11.6
Sikkim	39.4	39.5	0.2	0.4	4.1	−6.9	−0.8
Tamil Nadu	142.8	122.6	−20.2	−14.1	21.3	−21.7	1.9
Tripura	210.7	193.0	−17.7	−8.4	−0.6	−5.4	−2.8
Uttar Pradesh	79.1	58.4	−20.6	−26.1	1.9	54.1	25.4
West Bengal	203.9	198.5	−5.4	−2.6	7.2	12.3	9.5

[a] The following states and union territories are not represented: Andaman and Nicobar Islands, Dadra and Nagar Haveli, Chandigarh, Daman and Diu, Delhi and Pondicherry.
[b] Values averaged over each Indian state.

(2.4%) between the POT and IRR scenarios, while the change in domain-averaged water vapor was small (less than 0.5%).

Although our ensemble sensitivity analysis showed that model outputs were sensitive to the spatial scale of the analysis, we present changes in temperature (°C), moisture flux (g kg^{-1}) and planetary boundary layer (m) for the simulation over the entire South Asian domain in Fig. 9 for comparison with our previous analysis (Douglas et al., 2006). The spatial patterns are similar to those observed in Fig. 5 (original domain); the effect of intensive irrigation within Indo-Gangetic plain is striking. LH and SH mean values, averaged by Indian state for the POT and IRR scenarios, and the differences between these two scenarios (IRR mean minus POT mean) are shown in Tables 3a and 3b. The differences were considered to be statistically significant if the IRR mean value was outside of the 95% confidence interval for the POT mean value. Changes in latent heat fluxes (Table 3a) ranging from −20.6 to +37.2 Wm^{-2} (−26% to +24%) and sensible heat fluxes (Table 3b) ranging −87.5 to +4.4 Wm^{-2} (−77% to +8%) were found when model outputs were averaged over Indian states. Decreases in sensible heat in the states of Punjab (87.5 Wm^{-2} or 77%) and Haryana (65.3 Wm^{-2} or 85%) were found to be statistically significant at the 95% confidence level. In Table 3a, state-averaged IRR-POT LH differences are compared with seasonal and annual LH differences computed by the terrestrial water balance model (WBM; Vörösmarty et al., 1998) and presented in Douglas et al. (2006). The correlation between the RAMS LH differences and the WBM LH differences were positive but moderate: $r = 0.34$ for Kharif, and

Fig. 9. Changes in a) temperature (°C), b) water vapor (g kg^{-1}) and c) planetary boundary layer height (m) due to conversion of potential landcover to irrigated cropland for larger model domain.

Table 3b
Summary of sensible heat fluxes by Indian state estimated by RAMS over the larger domain. POT denotes the potential vegetation scenario, IRR denotes the irrigated agriculture scenario. The reduction in sensible heat fluxes for Haryana and Punjab (bold and italicized) was found to be statistically significant at the 95% confidence level.

State[a]	RAMS sensible heat (Wm^{-2})			
	POT[b]	IRR[b]	Difference[c]	%Change[d]
Andhra Pradesh	110.1	75.3	−34.8	−31.6
Arunachal Pradesh	24.3	22.1	−2.2	−9.1
Assam	11.6	10.7	−0.9	−8.0
Bihar	47.0	42.7	−4.2	−9.0
Gujarat	179.7	114.8	−64.9	−36.1
Haryana	***76.8***	***11.5***	***−65.3***	***−85.0***
Himachal Pradesh	28.9	31.5	2.6	9.0
Jammu and Kashmir	73.2	70.5	−2.7	−3.7
Karnataka	82.6	70.4	−12.2	−14.8
Kerala	55.7	60.0	4.4	7.9
Madhya Pradesh	62.4	37.2	−25.2	−40.4
Maharashtra	107.2	77.2	−30.0	−28.0
Manipur	27.0	26.0	−1.0	−3.7
Meghalaya	34.3	34.6	0.4	1.1
Mizoram	16.9	16.1	−0.9	−5.1
Nagaland	33.5	29.8	−3.7	−11.1
Orissa	27.4	31.4	4.0	14.5
Punjab	***113.2***	***25.7***	***−87.5***	***−77.3***
Rajasthan	156.1	93.1	−62.9	−40.3
Sikkim	4.4	5.9	1.5	33.2
Tamil Nadu	102.0	48.4	−53.6	−52.5
Tripura	3.1	0.0	−3.1	−100.0
Uttar Pradesh	30.8	12.8	−18.1	−58.6
West Bengal	58.8	36.8	−22.0	−37.4

[a] The following states and union territories are not represented: Andaman and Nicobar Islands, Dadra and Nagar Haveli, Chandigarh, Daman and Diu, Delhi and Pondicherry.
[b] Values averaged over each Indian state.
[c] Difference was computed as IRR minus POT.
[d] Percent difference relative to POT scenario.

$r = 0.43$ and 0.44 for Rabi and annual, respectively. This is likely due, at least in part, to differences in spatial resolution of the two models (5-minute in RAMS and 30-minute in WBM) and differences in how these models represent land–atmosphere (L–A) processes (L–A processes are coupled in RAMS, but de-coupled in WBM).

4. Summary and conclusions

The growth in human population has increased the demand for food supplies leading to intensified agriculture worldwide. The consequent changes in agricultural practices can lead to alterations in the landscape via changes in the land-use land-cover including irrigation. This study extended the hypothesis in Gordon et al. (2005) and Douglas et al. (2006) and has shown that irrigation and agricultural land use can alter the regional meteorology (and hence climate) by altering the moisture flux over the landmass. The study area is over India which has one of the highest rates of irrigation and agricultural intensification globally. The Regional Atmospheric Modeling System (RAMS) was configured over the Indian region and was able to successfully simulate the 16 to 20 July 2002 heavy precipitation event with an offshore low. In the control experiment, the NASA Global Inventory Modeling and Mapping Studies (GIMMS) efficiently provided the Normalized Difference Vegetation Index (NDVI) on 8 km grid increments which were blended to the RAMS domain with 25-km grid spacing. The first experiment considered the Global Land Cover GLC 2000 data with the control model configuration within RAMS to simulate the rain event. The model results were compared with various satellite and in situ data sources, including special observations available from a field experiment over the Arabian Sea. The domain-averaged bias was 14.2 mm, the spatial correlation (between the simulated and observed precipitation fields) was 0.59 (the model explained 34% of the variance) and the RMSE was quite high at 41.6 mm. These high errors have two main causes: 1) RAMS tends to overestimate precipitation and 2) the match between observed precipitation and precipitation in ECMWF data used as boundary conditions is also poor. Three additional experiments were performed with an identical model set up except with different land cover conditions: a potential land cover scenario (POT), a rainfed crop scenario (CRP) and an irrigated crop scenario (IRR). The 16 to 20 July 2002 case corresponds to a synoptic meteorological forced heavy rain event and yet results suggest that the changes in the agricultural landscape can alter the surface moisture and energy distribution, which can significantly affect the boundary layer and regional convergence, mesoscale convection and precipitation patterns.

Results indicate that the surface energy and moisture flux simulations over the Indian monsoon region are sensitive to the irrigation intensity and that this effect is more pronounced than the impact of land-use change from the potential vegetation to rainfed agricultural landscape. An ensemble sensitivity analysis revealed that sensible heat (SH) and water vapor (VP) were the least sensitive model outputs and that latent heat (LH) and precipitation (PR) were the most sensitive outputs in our analysis. Spatial discretization had the most dramatic affect on LH and PR but had little effect on SH and VP. When model outputs were averaged over the south Asia model domain, a statistically significant decrease in sensible heat flux between the potential vegetation and the irrigated agriculture scenarios of 11.7 Wm^{-2} was found. Changes in latent heat fluxes ranging from −20.6 to +37.2 Wm^{-2} (−26% to +24%) and sensible heat fluxes ranging −87.5 to +4.4 Wm^{-2} (−77% to +8%) were found when model outputs were averaged over Indian states. Decreases in sensible heat in the states of Punjab (87.5 Wm^{-2} or 77%) and Haryana (65.3 Wm^{-2} or 85%) were found to be statistically significant at the 95% confidence level. Differences in LH fluxes estimated by RAMS were positively but only moderately correlated with LH differences presented in Douglas et al. (2006), probably due, at least in part, to differences in spatial resolution of the two experiments and in how these models represent land–atmosphere (L–A) processes (L–A processes are coupled in RAMS, but de-coupled in WBM). Irrigation increased the regional moisture flux which in turn modified the convective available potential energy (CAPE), caused reduction in the surface temperature and led to a modified regional circulation pattern and changes in mesoscale precipitation. It is anticipated that agricultural changes, and irrigation impacts, can modify the regional climate and the mesoscale convection and rain patterns in the Indian monsoon region and need to be considered in multi-decadal climate variability and change assessments.

Acknowledgements

ECMWF ERA-40 data used in this study have been obtained from the ECMWF data server. The images and data used in this study were acquired using the GES-DISC Interactive Online Visualization ANd aNalysis Infrastructure (Giovanni) as part of the NASA's Goddard Earth Sciences (GES) Data and Information Services Center (DISC). This study benefited in part from support through NSF-ATM 0233780 (Dr. S. Nelson), NASA-THP NNG04GI84G (Dr. J. Entin), NASA-IDS NNG04GL61G (Drs. J. Entin and G. Gutman), NASA Land Use Land Cover Change Program (Dr. G. Gutman), and NASA grant NNX06AG74G.

References

Adegoke, J.O., Pielke Sr., R.A., Eastman, J., Mahmood, R., Hubbard, K.G., 2003. Impact of irrigation on midsummer surface fluxes and temperature under dry synoptic conditions: a regional atmospheric model study of the U.S. High Plains. Mon. Weather Rev. 131, 556–564.

Agrawal, S., Joshi, P.K., Shukla, Y., Roy, P.S., 2003. Spot-Vegetation Multi Temporal Data for Classifying Vegetation in South Central Asia. Indian Institute of Remote Sensing, vol. 4. Kalidas Road, Dehradun-248001, Uttaranchal (http://www-gvm.jrc.it/glc2000/Products/scasia/India_paper.pdf, accessed June 12, 2006).

Alpert, P., Niyogi, D., Pielke Sr., R.A., Eastman, J.L., Xue, Y.K., Raman, S., 2006. Evidence for carbon dioxide and moisture synergies from the leaf cell up to global scales: implications to human-caused climate change. Glob. Planet. Change 54, 202–208.
Avissar, R., Liu, Y., 1996. A three-dimensional numerical study of shallow convective clouds and precipitation induced by land surface forcing. J. Geophys. Res. 101, 7499–7518.
Bansil, P.C., 2004. Water Management in India. Concept Publishing Co., New Delhi.
Barnston, A.G., Schickedanz, P.T., 1984. The effect of irrigation on warm season precipitation in the southern Great Plains. J. Clim. Appl. Meteorol. 23, 865–888 (1984).
Beltrán, A.B. 2005,: Using a coupled atmospheric–biospheric modeling system (GEMRAMS) to model the effects of land-use/land-cover changes on the near-surface atmosphere. Ph.D. Dissertation. Department of Atmospheric Science, Colorado State University, 186 pp.
Boucher, O., Myhre, G., Myhre, A., 2004. Direct human influence of irrigation on atmospheric water vapour and climate. Clim. Dyn. 22, 597–604.
Castro, C.L., Cheng, W.Y.Y., Beltrán, A.B., Pielke Sr., R.A., Cotton, W.R., 2002. The incorporation of the Kain–Fritsch cumulus parameterization scheme in RAMS with a terrain-adjusted trigger function. Fifth RAMS Users and Related Applications Workshop. ATMET Inc., Santorini, Greece.
Castro, C.L., Pielke Sr., R.A., Leoncini, G., 2005. Dynamical downscaling: assessment of value retained and added using the Regional Atmospheric Modeling System (RAMS). J. Geophys. Res. Atmos. 110 (D5), D05108. doi:10.1029/2004JD004721.
Castro, C.L., Pielke Sr., R.A., Adegoke, J., Schubert, S.D., Pegion, P.J., 2007. Investigation of the summer climate of the contiguous U.S. and Mexico using the Regional Atmospheric Modeling System (RAMS). Part B: Model climate variability. J. Climate. 20, 3866–3887.
Central Water Commission (CWC), 1998. Water and Related Statistics. Central Water Commission, New Delhi, India.
Chen, C., Cotton, W.R., 1983. A one-dimensional simulation of the stratocumulus capped mixed layer. Boundary-Layer Meteor. 25, 298–321.
Cotton, W.R., Pielke, R.A., 2007. Human Impacts on Weather and Climate. Cambridge University Press. 330 pp.
Cotton, W.R., Pielke Sr., R.A., Walko, R.L., Liston, G.E., Tremback, C., Jiang, H., McAnelly, R.L., Harrington, J.Y., Nicholls, M.E., Carrio, G.G., McFadden, J.P., 2003. RAMS 2001: current status and future directions. Meteorol. Atmos. Phys. 82, 5–29.
Davis, M., 2001. Late Victorian Holocausts: El Niño Famines and the Making of the Third World. Verso1 85984 739 0. 464pp.
Douglas, E.M., Niyogi, D., Frolking, S., Yeluripati, J.B., Pielke Sr., R.A., Niyogi, N., Vörösmarty, C.J., Mohanty, U.C., 2006. Changes in moisture and energy fluxes due to agricultural land use and irrigation in the Indian Monsoon Belt. Geophys. Res. Lett. 33, L14403. doi:10.1029/2006GL026550.
Feddema, J.J., Oleson, K.W., Bonan, G.B., Mearns, L.O., Buja, L.E., Meehl, G.A., Washington, W.M., 2005. The importance of land-cover change in simulating future climates. Science 310 (5754), 1674–1678.
Gordon, L.J., Steffen, W., Jonsson, B.F., Folke, C., Falkenmark, M., Johannessen, A., 2005. Human modifications of global water vapor flows from the land surface. Proc. Natl. Acad. Sci. 102, 7612–7617.
Gupta, A.K., Anderson, D.M., Pandey, D.N., Singhvi, A.K., 2006. Adaptation and human migration, and evidence of agriculture coincident with changes in the Indian summer monsoon during the Holocene. Curr. Sci. 90, 1082–1090.
Holt, T., Niyogi, D., Chen, F., LeMone, M.A., Manning, K., Qureshi, A.L., 2006. Effect of land–atmosphere interactions on the IHOP 24–25 May 2002 Convection Case. Mon. Weather Rev. 134, 113–133.
Huffman, G.J., Adler, R.F., Morrissey, M.M., Bolvin, D.T., Curtis, S., Joyce, R., McGavock, B., Susskind, J., 2001. Global precipitation at one-degree daily resolution from multisatellite observations. J. Hydrometeorol. 2, 36–50.
Jha, S., 2001. Rainwater Harvesting in India. Press Information Bureau, Government of India, New Delhi, India. (http://pib.nic.in/feature/feyr2001/fsep2001/f060920011.html, accessed June 12, 2006).
Kabat, P., Claussen, M., Dirmeyer, P.A., Gash, J.H.C., Bravo de Guenni, L., Meybeck, M., PielkeSr. Sr., R.A., Vorosmarty, C.J., Hutjes, R.W.A., Lutkemeier, S. (Eds.), 2004. Vegetation, Water, Humans and the Climate: A New Perspective on an Interactive System. . Global Change — The IGBP Series. Springer, Berlin. 566 pp.
Kain, J.S., 2004. The Kain–Fritsch convective parameterization: an update. J. Appl. Meteorol. 43, 170–181.
Klemp, J.B., Wilhelmson, R.B., 1978. The simulation of three-dimensional convective storm dynamics. J. Atmos. Sci. 35, 1070–1096.
Krishnamurti, T.N., Biswas, M.K., 2006. Transitions in the surface energy balance during the life cycle of a monsoon season. J. Earth Syst. Sci. 115, 185–201.
Kuo, H.L., 1974. Further studies of the parameterization of the influence of cumulus convection on large-scale flow. J. Atmos. Sci. 31, 1232–1240.
Lohar, D., Pal, B., 1995. The effect of irrigation on premonsoon season precipitation over south west Bengal, India. J. Clim. 8, 2567–2570.
Marshall, C.H., Pielke Sr., R.A., Steyaert, L.T., 2004a. Has the conversion of natural wetlands to agricultural land increased the incidence and severity of damaging freezes in south Florida? Mon. Weather Rev. 132, 2243–2258.
Marshall, C.H., Pielke Sr., R.A., Steyaert, L.T., Willard, D.A., 2004b. The impact of anthropogenic land-cover change on the Florida peninsula sea breezes and warm season weather. Mon. Weather Rev. 132, 28–52.
Mellor, G.L., Yamada, T., 1982. Development of a turbulence closure model for geophysical fluid problems. Rev. Geophys. Space Phys. 20, 851–875.
Molinari, J., 1985. A general form of Kuo's cumulus parameterization. Mon. Weather Rev. 113, 1411–1416.
National Research Council, 2005. Radiative forcing of climate change: expanding the concept and addressing uncertainties. Committee on Radiative Forcing Effects on Climate Change, Climate Research Committee, Board on Atmospheric Sciences and Climate, Division on Earth and Life Studies. The National Academies Press, Washington, D.C. 208 pp.
Olson, D.M., Dinerstein, E., Wikramanayake, E.D., Burgess, N.D., Powell, G.V.N., Underwood, E.C., D'Amico, J.A., Itoua, I., Strand, H.E., Morrison, J.C., Loucks, C.J., Allnutt, T.F., Ricketts, T.H., Kura, Y., Lamoreux, J.F., Wettengel, W.W., Hedao, P., Kassem, K.R., 2001. Terrestrial ecoregions of the world: a new map of life on Earth. BioScience 51, 935–938.
Pielke, R.A., 1974. A three-dimensional numerical model of the sea breezes over south Florida. Mon. Weather Rev. 102, 115–139.
Pielke Sr., R.A., 2001. Influence of the spatial distribution of vegetation and soils on the prediction of cumulus convective rainfall. Rev. Geophys. 39, 151–177.
Pielke, R.A., Cotton, W.R., Walko, R.L., Tremback, C.J., Lyons, W.A., Grasso, L.D., Nicholls, M.E., Moran, M.D., Wesley, D.A., Lee, T.J., Copeland, J.H., 1992. A comprehensive meteorological modeling system — RAMS. Meteorol. Atmos. Phys. 49, 69–91.
Pielke Sr., R.A., Adegoke, J., Beltran-Przekurat, A., Hiemstra, C.A., Lin, J., Nair, U.S., Niyogi, D., Nobis, T.E., 2007a. An overview of regional land use and land cover impacts on rainfall. Tellus B 59, 587–601.
Pielke Sr., R.A., Adegoke, J.O., Chase, T.N., Marshall, C.H., Matsui, T., Niyogi, D., 2007b. A new paradigm for assessing the role of agriculture in the climate system and in climate change. Agric. For. Meteorol. 132, 234–254 (Special Issue).
Pielke, R.A., Marland, G., Betts, R.A., Chase, T.N., Eastman, J.L., Niles, J.O., Niyogi, D.D.S., Running, S.W., 2002. The influence of land-use change and landscape dynamics on the climate system: relevance to climate-change policy beyond the radiative effect of greenhouse gases. Philos. Trans. — Royal Soc., Math. Phys. Eng. Sci. 360 (1797), 1705–1719.
Pinzón, J.E., 2002. Using HHT to Successfully Uncouple Seasonal and Interannual Components in Remotely Sensed Data. SCI, Orlando, Florida. 2002.
Pinzón, J.M., Brown, M., Tucker, C.J., 2004. Satellite time series correction of orbital drift artifacts using empirical mode decomposition. In: Huang, N. (Ed.), Hilbert-Huang Transform: Introduction and Applications.
Pitman, A.J., 2003. The evolution of, and revolution in, land surface schemes designed for climate models. Int. J. Climatol. 23, 479–510.
Rao, P.S., Sikka, D.R., 2005. Intraseasonal variability of the summer monsoon over the North Indian Ocean as revealed by the BOBMEX and ARMEX field programs. Pure Appl. Geophys 162 (8–9), 1481–1510. doi:10.1007/s00024-005-2680-0.
Roy, S.B., Hurtt, G.C., Weaver, C.P., Pacala, S.W., 2003. Impact of historical cover change on the July climate of the United States. J. Geophys. Res. 108, 4793. doi:10.1029/2003/JD003565, 2003.
Saleeby, S.M., Cotton, W.R., 2004. Simulations of the North American monsoon system. Part I: model analysis of the 1993 monsoon season. J. Climate 17, 1997–2018.
Sellers, P.J., Los, S.O., Tucker, C.J., Justice, C.O., Dazlich, D.A., Collatz, G.J., Randall, D.A., 1996. A revised land surface parameterization (SiB2) for atmospheric GCMs. Part II: the generation of global fields of terrestrial biophysical parameters from satellite data. J. Climate 9, 706–737.
Smagorinsky, J., 1963. General circulation experiments with the primitive equations. Part I: the basic experiment. Mon. Weather Rev. 91, 99–164.
Tucker, C.J., Pinzón, J.E., Brown, M.E., Slayback, D., Pak, E.W.W., Mahoney, R., Vermote, E., El Saleous, N., 2005. An extended AVHRR 8-km NDVI data set compatible with MODIS and SPOT vegetation NDVI Data. Int. J. Remote Sens. 26, 4485–4498.
Uppala, S.M., Kållberg, P.W., Simmons, A.J., Andrae, U., Da Costa Bechtold, V., Fiorino, M., Gibson, J.K., Haseler, J., Hernandez, A., Kelly, G.A., Li, X., Onogi, K., Saarinen, S., Sokka, N., Allan, R.P., Andersson, E., Arpe, K., Balmaseda, M.A., Beljaars, A.C.M., Van De Berg, L., Bidlot, J., Bormann, N., Caires, S., Chevallier, F., Dethof, A., Dragosavac, M., Fisher, M., Fuentes, M., Hagemann, S., Hólm, E., Hoskins, B.J., Isaksen, L., Janssen, P.A.E.M., Jenne, R., McNally, A.P., Mahfouf, J.F., Morcrette, J.J., Rayner, N.A., Saunders, R.W., Simon, P., Sterl, A., Trenberth, K.E., Untch, A., Vasiljevic, D., Viterbo, P., Woollen, J., 2005. The ERA-40 re-analysis. Quart. J. R. Meteorol. Soc. 131, 2961–3012.
Vörösmarty, C.J., Federer, C.A., Schloss, A.L., 1998. Potential evaporation functions compared on US watersheds: possible implications for global-scale water balance and terrestrial ecosystem modeling. J. Hydrol. 207, 147–169.
Vörösmarty, C.J., Leveque, C., Revenga, C., Caudill, C., Chilton, J., Douglas, E.M., Meybeck, M., Prager, D., 2005. Chapter 7: fresh water. Conditions and Trends Working Group Report. Millennium Ecosystem Assessment, vol. 1. Island Press.
Walko, R.L., Band, L.E., Baron, J., Kittel, T.G.F., Lammers, R., Lee, T.J., Ojima, D.S., Pielke, R.A., Taylor, C., Tague, C., Tremback, C.J., Vidale, P.L., 2000. Coupled atmosphere–biophysics–hydrology models for environmental modeling. J. Appl. Meteorol. 39, 931–944.
Willmott, C.J., Feddema, J.J., 1992. A more rational climatic moisture index. Prof. Geogr. 44, 84–87.
Zickfeld, K., Knopf, B., Petoukhov, V., Schellnhuber, H.J., 2005. Is the Indian summer monsoon stable against global change? Geophys. Res. Lett. 32. doi:10.1029/2005GL022771.